OSNAP technical report

Calculation method summary

01.05.2023

Yao Fu[1], Feili Li[2], William E. Johns[3], M. Susan Lozier[1]

[1]Georgia Institute of Technology

[2]Xiamen University

[3]University of Miami

Table of Content

Introduction

The Overturning in the Subpolar North Atlantic Program (OSNAP) observing system utilizes data from a suite of moorings, gliders, Argo floats, and satellite altimetry to estimate the subpolar Atlantic Meridional Overturning Circulation (MOC). The OSNAP section consists of two parts: OSNAP West extends from southern Labrador to southwestern Greenland and OSNAP East from southeastern Greenland to the coast of Scotland (Fig. 1). Since 2014 OSNAP array have been continuously monitoring the MOC, as well as the meridional heat (MHT) and freshwater (MFT) transports in the subpolar North Atlantic. Currently, the OSNAP record is 71 months (August 2014 to June 2020). Results have been published and the data is freely available at https://www.o-snap.org/data-access/.

In this technical report, we synthesize the OSNAP MOC metrics calculation methods that have been documented in a series of OSNAP publications. The readers are referred to the papers listed in **References** for more details.

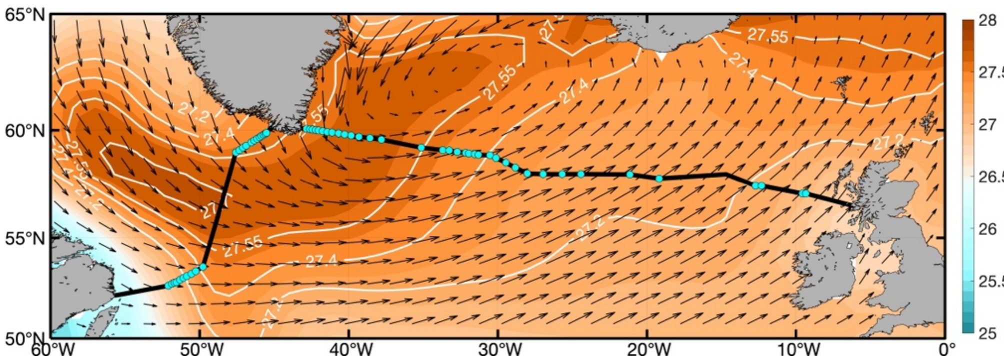

Figure 1 OSNAP Section. Winter (January to March) climatological wind stress from ERA5 (2014-2020) over the subpolar North Atlantic (vectors, in N m^{-2}) superimposed on climatological winter sea surface density from EN4 (shading with contours, in kg m^{-3}, for 2014-2020). OSNAP West and OSNAP East sections are indicated by black lines with OSNAP mooring positions denoted with cyan dots.

Current calculation methods

This section synthesizes the up-to-date calculation methods for the OSNAP metrics based on the 71-month OSNAP observations, as described in Lozier et al. (2019), Li et al. (2021a) and Fu et al. (2023).

MOC, MHT and MFT calculations

The MOC (Fig. 2) is defined as the maximum of the overturning stream function, Ψ, in potential density (σ_θ) space as:

$$\text{MOC}(t) = \max[\Psi(\sigma, t)] = \max\left[\int_{\sigma_{min}}^{\sigma_{max}} \int_{x_w}^{x_e} v(x, \sigma, t) dx d\sigma\right], \quad (1)$$

where v is the cross-sectional volume transport per unit length per unit density along the OSNAP section (positive poleward), which is integrated from west (x_w) to east (x_e) and from the smallest density surface (σ_{min}) to the largest (σ_{max}) throughout the water column. The velocity field along the OSNAP section is derived using a combination of direct velocity measurements and geostrophic calculation based on the thermal wind relation. The density at which the overturning stream function reaches the maximum is σ_{MOC}. The MOC upper (lower) limb transport is the transport above (below) σ_{MOC} in the overturning stream function. The 2014-2020 mean MOC is 16.7±0.6 Sv with mean σ_{MOC} of 27.63 kg m^{-3} across the full OSNAP section, 16.3±0.6 Sv with 27.54 kg m^{-3} across OSNAP East, and 3.0±0.5 Sv with 27.69 kg m^{-3} across OSNAP West.

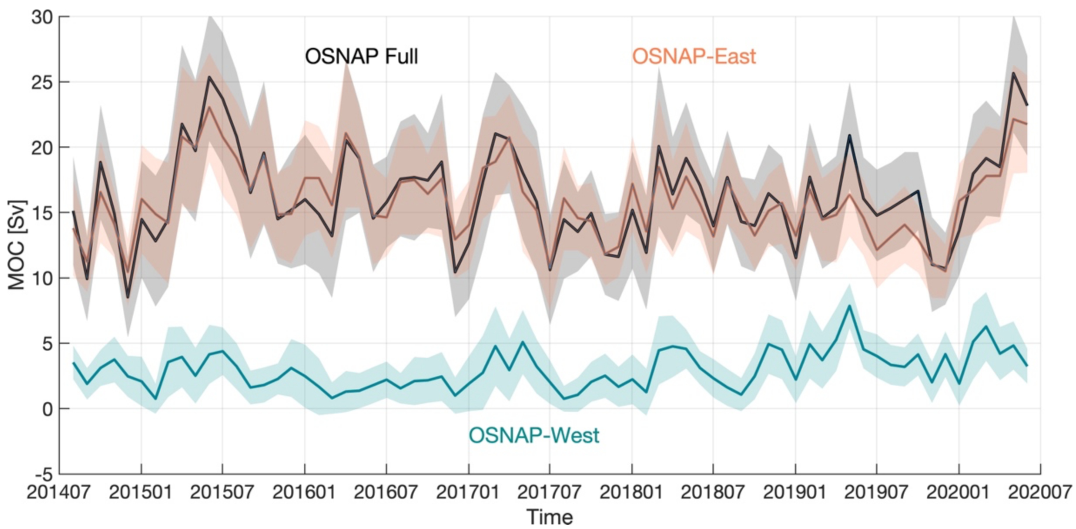

Figure 2 Meridional Overturning Circulation (MOC) time series. Monthly MOC time series across the full OSNAP array (black), OSNAP East (orange), and OSNAP West (cyan). Shading indicates monthly uncertainty estimated from a Monte Carlo analysis (Lozier et al. 2019).

MHT (Fig.3a) is defined as:

$$\text{MHT}(t) = \rho C_p \int_{\sigma_{min}}^{\sigma_{max}} \int_{x_w}^{x_e} v(x, \sigma, t)\theta(x, \sigma, t) dx d\sigma, \quad (2)$$

where ρ is potential density, C_p is the specific heat of seawater and θ is potential temperature.

MFT (Fig. 3b) is defined as:

$$\text{MFT}(t) = -\int_{\sigma_{min}}^{\sigma_{max}} \int_{x_w}^{x_e} v(x, \sigma, t) \frac{S(x, \sigma, t) - \bar{S}}{\bar{S}} dx d\sigma, \quad (3)$$

where S is salinity, and $\bar{S}$ is the area-weighted section mean salinity (34.92 across the full OSNAP section). Note that MFT is defined following Lozier et al. (2019) and should be regarded as an equivalent oceanic freshwater transport due to meridional salinity transport (also see Li et al., 2021b for more details).

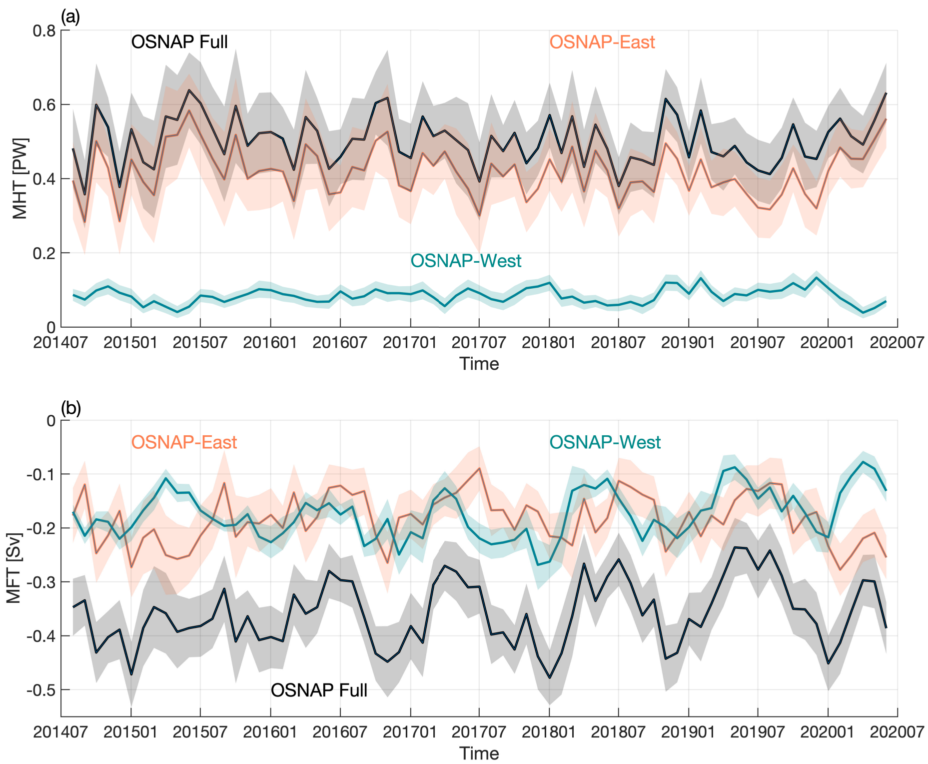

Figure 3 Meridional heat and freshwater transport time series. Monthly MHT (a) and MFT (b) across the full OSNAP array (black), OSNAP East (orange), and OSNAP West (cyan). Shading indicates the monthly uncertainty estimated using a Monte Carlo analysis (Lozier et al. 2019).

Property and velocity fields

Property and velocity fields are calculated on a grid along the OSNAP section. The grid uses a Cartesian coordinate system with the x-axis parallel to the OSNAP line passing through all moorings, the y-axis perpendicular to that line, and the positive z-axis pointing upward. The horizontal resolution of this grid is ~1/4° and the vertical resolution is uniformly 20 m.

Mooring data in the boundary arrays are interpolated to estimate the temperature, salinity and density fields in these areas. Away from the arrays, gridded property fields are produced down to 2000 m via an objective analysis method based on temperature and salinity from Argo profiles, OSNAP gliders and moorings, and World Ocean Atlas 2013 (WOA13) temperature and salinity climatology. The WOA13 data are also used in the unmeasured areas on the Labrador and Scottish shelves (Figure 2 of Li et al., 2017). Details on the validation of the objective analysis method can be found in previous studies. Below 2000 m, hydrographic data from 407 OSNAP CTD stations occupied during the summers of 2014 and 2016 are used to fill the grid. See complete cruise information at http://www.o-snap.org/observations/research-cruises/.

Mooring velocity data are interpolated to determine the velocity field in the boundary arrays. Away from the arrays, Ekman velocities calculated using ERA5 wind stress are added to the surface Ekman layer, and geostrophic velocities are calculated with two different choices of reference depending on the availability of deep moorings. Where available, directly measured velocities at the top of deep moorings are used to provide the reference, with two exceptions: one in the western Labrador Basin and one in the central Iceland Basin. There, and in areas without deep moorings, the time-mean surface velocity from satellite altimetry is used as the reference velocity. Because of the uncertainties of the surface velocities derived from satellite altimetry in the region, we use the altimetry-derived velocities to calculate a mean reference velocity only. For each time step, we use this mean reference velocity (only in the areas where we have no direct velocity measurements from moorings) and allow a compensation transport to determine the time-varying barotropic velocity.

For the unmeasured flow on the Labrador and Scottish shelves (see Figure 2 in Li et al., 2017), we use an ensemble-mean velocity climatology for 46 months, which is derived from three ocean or ocean-sea-ice models and one ocean reanalysis. This is to reduce a potential transport bias from any specific model.

Net throughflow

Our calculation assumes a zero net meridional mass transport across the entire OSNAP section. Long-term measurements across Davis Strait show a mean transport of -1.6 ± 0.2 Sv from the Arctic into the North Atlantic. To account for this transport, and still satisfy a zero-net-mass constraint across the entire section, we allow for a net transport of -1.6 ± 0.2 Sv across OSNAP West and then add a compensating transport of the same magnitude but with opposite sign across OSNAP East. When calculating the MOC at OSNAP West and East separately, we apply these same constraints.

Compensation transport

A compensation transport (Fig. 4) is added at each time step to ensure a zero net meridional mass transport across the entire OSNAP section. That is, we use the constraint of zero net meridional mass transport to identify the fluctuating barotropic component of the flow. The mean compensation transport across the full array and its uncertainty (standard error, with 22 effective degrees of freedom) over the 71-month observational period is -2.9 ± 1.8 Sv. This mean compensation transport is equivalent to adding a spatially uniform velocity of -0.07 cm/s across OSNAP West and -0.05 cm/s across OSNAP East to those areas without direct velocity measurements. The compensation velocity varies in time: the standard deviation of its time mean is 0.22 cm/s for OSNAP West and 0.32 cm/s for OSNAP East. The compensation transport is not significantly correlated with the MOC across the full array with a correlation coefficient of 0.18 based on the 71-monthly OSNAP observations.

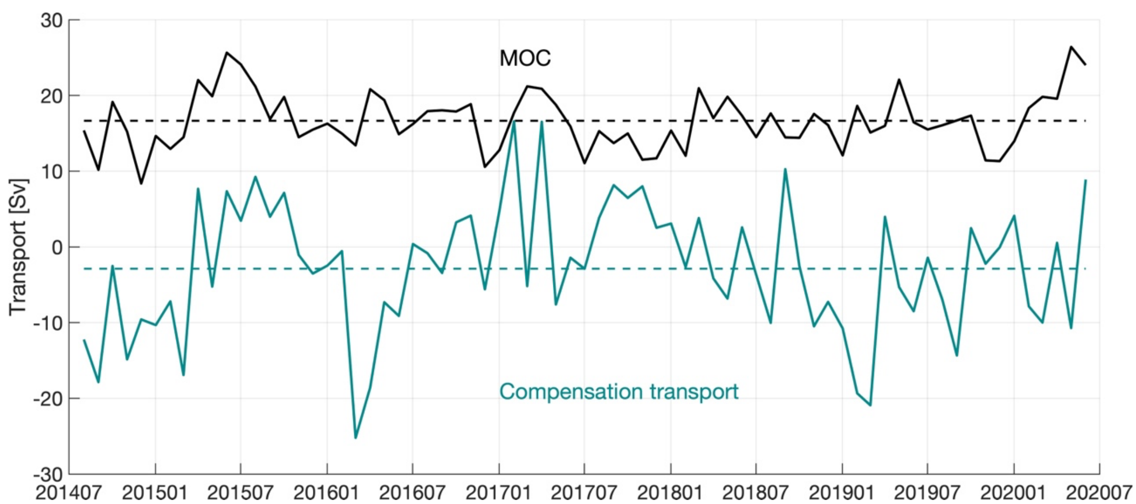

Figure 4 Compensating transport (cyan) and MOC (black) across the full OSNAP array

Monthly mean and uncertainty estimates

We use Monte Carlo simulations to calculate estimates of the mean fluxes and to provide an estimate of the statistical uncertainty in those means. The statistical uncertainty stems from the intrinsic transport variability and random measurement uncertainty, and is typically dominated by the former. We note that all reported uncertainties indicate statistical uncertainty, and do not include possible bias errors, i.e., errors due to biases in Ekman transport or to deficiencies in array design or calculation methodology. A possible bias error of up to ~10% of the mean was found in

Li et al. (2017) based on Observing System Simulation Experiments (OSSEs) using a global ocean–sea-ice model. Further analysis will be performed for evaluating possible bias error at OSNAP and its sources.

For each monthly period: We first create a field of variables used for the MOC, MHT and MFT estimates using the local (i.e., at each instrument site) monthly mean and standard error for each variable at that site. These variables are temperature, salinity, velocity, sea surface height, wind stress, and the net throughflow across the subsection. For each Monte Carlo iteration, we randomly draw from these distributions to produce one realization of MOC (similarly for MHT and MFT). We continue the Monte Carlo iterations until the running mean of the flux estimate converges to within a prescribed value, ϵ, at which point the standard deviation of the mean has also converged ($\epsilon = 1 \times 10^{-3}$ Sv for MOC, 2×10^{-5} PW for MHT and 2×10^{-5} Sv for MFT). We use the average of all iterations as the mean flux for each monthly period and report the standard deviation of the average as the uncertainty. Uncertainty in the monthly mean estimates is ~ 4 Sv for MOC, 0.1 PW for MHT and 0.1 Sv for MFT.

Uncertainty estimates for the time-mean MOC, MHT and MFT

The standard error of the 71-month mean MOC, MHT and MFT is used as the uncertainty of the time-mean values. The standard error is calculated as:

$$SE = \frac{STD}{\sqrt{DOF}}, \qquad (4)$$

where *STD* represents the standard deviation of a quantity (i.e., the MOC, MHT and MFT) based on the corresponding monthly time series. *DOF* is the effective number of degrees of freedom, which is calculated as the total length of a time series divided by the decorrelation timescale. The decorrelation timescale is determined as the integral of the corresponding autocorrelation function between the first positive and negative zero-crossings. We estimate that there are 43, 30 and 13 independent values in the 71-month MOC time series for the full array, OSNAP East, and OSNAP West, respectively.

Decomposition of MHT and MFT into overturning and isopycnal components

The MHT and MFT across each OSNAP section are decomposed into overturning and isopycnal components by first defining the total velocity, potential temperature and salinity as:

$$v(x,\sigma,t) = <v> (\sigma,t) + v'(x,\sigma,t)\ [m\ s^{-1}], \qquad (5)$$

$$\theta(x,\sigma,t) = <\theta> (\sigma,t) + \theta'(x,\sigma,t)\ [°C], \qquad (6)$$

$$S(x,\sigma,t) = <S> (\sigma,t) + S'(x,\sigma,t), \qquad (7)$$

where the angle brackets indicate a horizontal average at constant density and the prime indicates deviations from that average.

The MHT across each OSNAP section can then be divided into an overturning, $MHT_{overturning}$, and 'isopycnal' component, $MHT_{isopycnal}$ as follows:

$$MHT_{overturning}(t) = \rho C_p \int_{\sigma_{min}}^{\sigma_{max}} \int_{x_w}^{x_e} <v> (\sigma,t) <\theta> (\sigma,t) dx d\sigma\ [W], \qquad (8)$$

$$MHT_{isopycnal}(t) = \rho C_p \int_{\sigma_{min}}^{\sigma_{max}} \int_{x_w}^{x_e} v'(x,\sigma,t)\theta'(x,\sigma,t) dx d\sigma\ [W], \qquad (9)$$

where $\rho C_p = 4.1 \times 10^6\ Jm^{-3}K^{-1}$, and the double integral is taken over all σ surfaces and between the western and eastern boundaries.

The MFT across each OSNAP section is similarly decomposed:

$$MFT_{overturning}(t) = -\int_{\sigma_{min}}^{\sigma_{max}} \int_{x_w}^{x_e} <v> (\sigma,t) \frac{<S> (\sigma,t)}{\bar{S}} dx d\sigma\ [Sv], \qquad (10)$$

$$MFT_{isopycnal}(t) = -\int_{\sigma_{min}}^{\sigma_{max}} \int_{x_w}^{x_e} v'(x,\sigma,t) \frac{S'(x,\sigma,t)}{\bar{S}}\ dx d\sigma\ [Sv]. \qquad (11)$$

Ekman transport calculation

The cross-sectional Ekman transport for the OSNAP section, M_{Ek}^{y}, is calculated from ERA5 surface wind stress as:

$$M_{Ek}^{y} = -\frac{1}{\rho_0}\frac{\tau_x}{f}, \qquad (12)$$

where ρ_0 is the density of sea water with a constant value of 1,025 kg m^{-3}, τ_x is the wind stress projected along the OSNAP section, and f is the Coriolis parameter. The Ekman transport is applied to the OSNAP section where there is no direct velocity measurement near the surface and within the theoretical Ekman layer. The section-mean Ekman layer depth is about ~25 m.

The zero net volume transport constraint across the full OSNAP section requires the surface-layer Ekman transport to be balanced by an instantaneous barotropic return flow that is evenly distributed across the full section. In the calculation of the MOC, MHT and MFT without Ekman transport components, we removed the Ekman transport in the Ekman layer and the Ekman return flow from the derived velocity field at each time step.

Ekman transport across OSNAP East dominates the mean and variability of the total Ekman transport across the full array. This dominance can be attributed to the fact that the orientation of the OSNAP East section is almost parallel to the westerly winds, which generates large cross-sectional Ekman transport. To test the sensitivity of the Ekman transport strength to the latitudinal location of the OSNAP East, we randomly shifted the entire OSNAP East section within 1° latitude to the north or south of its current position. These runs yielded mean Ekman transports within 0.1 Sv of the mean Ekman transport (-1.7±0.3 Sv) across the current line, leading us to conclude that sensitivity to local latitudinal variability is weak.

Water mass transformation rate

Following previous studies, the rate of water mass transformation, F, is calculated by integrating surface density fluxes induced by air-sea buoyancy fluxes over the outcropping area of a given isopycnal as:

$$F(\sigma^*) = \frac{1}{\Delta\sigma}\iint \left[-\frac{\alpha}{C_p}Q + \beta\frac{S}{1-S}(E-P)\right]\prod \sigma \, dxdy, \qquad (13)$$

where

$$\prod \sigma = \begin{cases} 1 & \text{for } [\sigma-\sigma^*] \le \frac{\Delta\sigma}{2} \\ 0 & \text{elsewhere.} \end{cases}$$

In Eq. (13), α and β are the thermal expansion and haline contraction coefficients, respectively. Q is the net heat flux into the ocean, and S is the surface salinity. E and P are the evaporation and precipitation rates, respectively. $\Delta\sigma = 0.2$ kg m^{-3} is the density bin size that the outcropping density (σ^*) represents. Positive transformation indicates conversion of water lighter than the specified isopycnal to water denser than the isopycnal. The Labrador Basin is defined as the area enclosed by the 2000-m isobath of the Labrador Sea and the OSNAP West line. Using the 2000-m isobath excludes the shallow continental shelf region along the Labrador coast, where water is much lighter than mean σ_{MOC} of 27.69 kg m^{-3} in the Labrador Sea. The continental slope on both sides of Greenland is very steep. Using the coastline or 2000-m isobath has negligible impact on the outcropping area. The eastern subpolar gyre is defined as the area between the OSNAP East section and the Greenland-Scotland-Ridge.

The National Centers for Environmental Prediction Climate Forecast System v2 (NCEP/CFSv2) heat and freshwater fluxes and Roemmich-Gilson Argo Climatology monthly temperature and salinity from January 2014 to December 2020 are used to calculate the transformation. Using a different combination of datasets, for example, NCEP/CFSv2 heat and freshwater fluxes with surface temperature and salinity derived from the Met Office EN4, results in a qualitatively similar transformation seasonal cycle, with the same phase yet a slightly different winter transformation. Specifically, the December-to-March mean transformation (±standard deviation) for the eastern subpolar gyre is 10.7±1.9 Sv and 11.8±1.8 Sv for the Argo-based and EN4-based calculations, respectively. The values for the western subpolar gyre are 4.6±2.8 Sv and 4.3±1.9 Sv for the Argo-based and EN4-based calculations, respectively. Given the similarity of these estimates, we use the combination of NCEP/CFSv2 and Argo to demonstrate the seasonal cycle of water mass transformation.

Monthly climatology calculation

The climatological mean MOC, MHT and MFT for each month from January to December are calculated based on the 71-month OSNAP observations that cover the period from August 2014 to June 2020. For January to June and August to December, there are 6 monthly realizations during the 71-month observational period. For July, there are only 5 monthly values during the same period. The monthly climatology is calculated by averaging the available realizations of each month. The standard error of the monthly climatological mean is used as the uncertainty and is calculated as the standard deviation divided by the square root of the number of available realizations of each month (i.e., 5 for July and 6 for the other months).

History of calculation updates

This section describes a sequence of updates in the MOC, MHT, and MFT calculation since the publication of Lozier et al. (2019). The updates are listed in the order of time. Unless stated, the updates applied in previous publications are also adopted in the following publications. Some updates may be publication-specific in terms of the length of data used for the tests. Please refer to the indicated publication for the impacts of any update on the MOC, MHT and MFT calculation.

Li et al. (2021a):

There have been a couple of updates in the calculations since Lozier et al.10which are related to changes in the array configuration (e.g., addition or loss of instruments) or in the auxiliary data pro-ducts. Those changes affect the calculations of the cross-sectional velocity field, and, to a lesser extent, the MOC estimate when integrating over the whole section. Here we describe individual changes generally from west to east, and assess their impact on the MOC by comparing the estimates with and without one specific change implemented. The time period over which the assessment is performed depends on the data availability, which ranges from 8 to 46 months (the maximum length of the observational record). All test runs have been conducted using the 30-day averaged data.

Updated velocity climatology for the Labrador shelf current (LSC). The LSC is an unmeasured component at OSNAP West that flows southward at water depth shallower than ~300 m (Fig.1 in Li et al., 2021a for location). It carries the freshest and coldest waters in the subpolar region ($\theta \approx 0.8$ °C and $S \approx 33.6$), constituting a major component of the freshwater flux across the section. In Lozier et al. (2019) monthly climatological velocities from a high-resolution (1/12°) regional ocean circulation model (FLAME) were used for representing the LSC at OSNAP. In the current calculations, we have used an ensemble-mean velocity climatology for the whole length of the record (46 months), which is derived from three ocean or ocean-sea-ice models and one ocean reanalysis (Supplementary Table 1). This is to reduce a potential transport bias from any specific model. In addition, World Ocean Atlas 2018 (WOA18) temperature and salinity climatology were used to replace WOA13.

The LSC transport shows very similar magnitudes among the four products with a shared seasonality that is strong in winter and weak in summer (not shown). The ensemble-averaged annual-mean LSC transport (-2.6 Sv) is slightly stronger than the transport in FLAME (-2.4 Sv). The LSC contains the lightest waters across the section and a stronger LSC transport (southward) causes a weaker transport in the upper MOC limb (northward). The comparison of the MOC estimates during 2014-2018 shows that using the ensemble-mean velocity climatology yields a reduction in the mean MOC by 0.2 Sv, compared to that using FLAME only.

Inclusion of the data from three RREX moorings. Three tall moorings that were part of the RREX array48were deployed in the summer of 2015 right on the OSNAP line in the eastern Irminger basin (Fig.1 in Li et al., 2021a). They had been continuously measuring temperature, salinity and velocity throughout the water column for 2 years (from29-Jun-2015 to 26-Jul-2017). The RREX moorings are situated between four existing OSNAP moorings, designed to capture the property and velocity structures of the northward-flowing Irminger Current (IC) above the western flank of the Reykjanes Ridge. The RREX mooring data were retrieved in the summer of 2017 and thus none of them were included in our first 21-month OSNAP time series. In the current calculations, we have incorporated the RREX mooring data in the property and velocity interpolations in the region whenever they are available. To assess the impact on the flux estimate, we compared the transports calculated with and without the RREX mooring data during the 2-year RREX period. The comparisons show that using the RREX data yields a small increase in the mean IC transport (0.8 Sv or ~10% of the mean transport). Because the IC comprises waters in both the upper and lower MOC limbs, the corresponding impact on the MOC estimate is smaller. Over the 2015–2017 time period, the inclusion of the RREX mooring data results in an increase in the time-mean MOC by 0.2 Sv.

Modified reconstruction of the deep current in the Iceland basin. The deep current in the western Iceland basin contains the densest overflow waters in the subpolar North Atlantic flowing southward across the OSNAP East section. The deep current has a bottom velocity core above the eastern flank of the Reykjanes Ridge with a clear intrusion farther into the basin interior (Fig.1b). Our modification of the calculation method is concerning the reconstruction of the interior transport, i.e., water deeper than ~2200 m and between 28.0 and 24.4°W (between the M2 and IB3 moorings). In Lozier et al. (2019) the bottom velocity field was derived based on the measurements from M2 and IB3 along with D4 in the following way: velocities from M2 and D4 were interpolated to fill the area between them, while geostrophic velocities were calculated between D4 and IB3. In the current calculations, we have modified the method by disregarding the velocity interpolations and instead calculating the geostrophic flow between M2 and IB3 for the whole 2014-2018 time period. Because the M2 mooring is at a water depth (~2400 m) shallower than IB3 (~2800 m), we added the temperature and salinity measurements from the deepest instrument from D4 (at ~2600 m) to M2. It effectively minimizes the bottom triangle below the maximum common depth between the moorings M2 and IB3. To assess the impact from this change, we compared the transport of bottom waters ($\sigma_\theta > 27.80$ kg m^{-3}) between M2 and IB3 for the whole 46-month time period. It shows that the new method yields a small reduction in the time-mean transport in the bottom layer (0.5 Sv) which leads to a reduction in the time-mean MOC by 0.2 Sv.

Updated objective analysis (OA) product. Away from the boundary arrays, temperature and salinity fields are created based primarily on the Argo and mooring data in the vicinity, using an OA technique. In Lozier et al. (2019), OA was performed on depth surfaces (OA_{depth}), which inevitably tends to mix waters with different densities. In the current calculations, we have used OA gridded products where OA is performed on density surfaces (OA_{dens}) to best preserve water properties. This updated product was used throughout the 2014-2018 time period. Input for the OA_{dens} comprises the Argo data, OSNAP mooring data as well as the WOA18 climatology. Note that OA_{dens} is limited to the upper water column owing to the limitation of the maximum sampling depth of Argo floats (2000 m). For the deeper layers, we use hydrographic data from the 2014 and 2016 summer OSNAP cruises. Density fields are calculated from gridded temperature and salinity fields using Gibbs Seawater Oceanographic Toolbox (version 3.06.11) of the International Thermodynamic Equation of Seawater-2010 (TEOS-10).

The OA_{dens} impact on the MOC estimate mainly arises from the use of density profiles for calculating the geostrophic flow in the glider survey domain above the Hatton-Rockall Plateau (Fig.1 in Li et al. 2021a), which is associated with the northward North Atlantic Current (NAC) transport in the upper MOC limb. To assess the impact, we calculated the transports with OA_{depth} and OA_{dens}, respectively, for the whole 46-month observational period. The comparisons between those two estimates reveal an increase of ~1 Sv in the time-mean NAC transport in the region when using OA_{dens}, with an increase in the time-mean MOC of 1.2 Sv.

Time-mean transport in the eastern Rockall Trough wedge. In the easternmost part of the OSNAP section, there is a strong northward-flowing shelf-break current (~1 Sv) in the eastern wedge of the Rockall Trough (Fig.1). An upward-looking ADCP (acoustic Doppler current profiler) was mounted at the ~500 m water depth for capturing this wedge transport. However, due to multiple instrument losses, there has been only ~8 months of good data returned (30-Oct-2014 to 19-June-2015) during the whole 4-year deployment.

To accommodate this data loss, in Lozier et al. (2019) velocities from the nearest current meter mooring (RTEB1) to the ADCP were used to fill the wedge when the ADCP data are not available. To assess its impact (e.g., to what extent it captures the shelf-break current), the transports were calculated using the RTEB1 data following Lozier et al. (2019) during the 8-month time period when the ADCP data are available. Comparing it to the actual ADCP-derived transport suggests that using the RTEB1 data does not resolve the 1 Sv mean wedge transport. Because the transport is within the upper MOC limb, such an underestimation leads to an underestimation in the MOC of 0.8 Sv in the mean MOC during the same 8-monthperiod. Thus, using the time-mean ADCP velocity for all the times when no ADCP data are returned leads to an increase in the time-mean MOC of 0.8 Sv.

Updated time-mean altimetry reference velocity. As part of the velocity calculations, the time-mean surface velocity over the observational record from satellite altimetry is used to provide the surface reference for calculating the absolute geostrophic velocities in the basin interior. With the extension of the length of our records, we have now used 4-year mean altimetry velocity (23-Aug-2014 to 26-May-2018) in the current calculations. To assess the impact from this update, we compare the MOC estimates for the 2014-2018 time period using the time-mean surface velocity averaged over the first 21 months and over the whole 46 months, respectively. It shows a reduction in the time-mean MOC by 0.4 Sv with the 46-month mean altimetry reference. Note that in contrast to the other updates, the impact from the change in the reference velocity will be reduced with alonger record (i.e., when the change in the length of the record becomes relatively small compared to the length of record itself).

Impact on MOC estimates. The change in the mean MOC estimate is not a simple sum of all the changes caused by the individual updates listed above, because updates impact the velocity and MOC during certain times of the observational period. Overall, the updates have changed the time-mean MOC during the first 21-month period from 14.9±1.0 Sv to 16.5±1.0 Sv, with negligible impact on the variability (r=0.97). However, the difference in the mean MOC estimates is not statistically significant according to their standard errors.

Fu et al. (2023):

Several updates have been implemented in the MOC calculations since Li et al. (2021a) with respect to the configuration of the OSNAP array (i.e., adding or removing moorings), averaging window of the time series, and recalibration of instruments. These updates impact the calculation of the cross-sectional velocity field, which marginally changes the MOC that is calculated based on the cross-sectional velocity (Eq. 1). Here we document each change and evaluate the impact of this change on the MOC by comparing the MOC estimates with and without this specific change. The updates below apply to the 71-month OSNAP observations from August 2014 to June 2020.

Averaging window. In the previous OSNAP calculations, the MOC is calculated using 30-day averaged mooring and auxiliary data (e.g., Argo temperature and salinity profiles, wind, sea surface height, etc.), resulting in a MOC time series with 30-day temporal resolution. As the OSNAP observations have been extended to ~6 years and will continue to a longer period, the 30-day averaging window will, in time, lead to a growing misalignment between the 30-day time series and the calendar months. Therefore, from this study onward, the MOC is calculated using monthly-averaged mooring and auxiliary data to obtain an OSNAP time series aligned with calendar months, currently from August 2014 to June 2020. Since the MOC time series is calculated based on either monthly-averaged or 30-day-averaged mooring and auxiliary data, a negligible difference of 0.02 Sv is detected in the 6-year mean for the full OSNAP array. However, when the monthly and 30-day MOC time series are derived from the same daily MOC time series, they have an identical time-mean value.

Ekman transport calculation. In the previous OSNAP metrics calculation, the Ekman transport across the full OSNAP section is calculated using wind stress derived from European Centre for Medium-Range Weather Forecasts (ECMWF) ERA5 wind speed using a bulk formula. Since ERA5 directly provides wind stress data, the Ekman transport is directly calculated using the ERA5 wind stress from this study onward. Compared to the previous calculation, using the ERA5 wind stress decreased mean MOC across the full array by only 0.06 Sv, which is much smaller than the uncertainty range.

Inclusion of the data from moorings LSA and LSB on the West Greenland shelf. Two additional moorings, LSA and LSB, were deployed in September of 2018 at the eastern end of the OSNAP West line to measure the inshore West Greenland Coastal Current and its water properties. The West Greenland Coastal Current carries the freshest coastal water northward into the Labrador Sea along the eastern coast. The two moorings continuously measure current velocity, temperature and salinity throughout the water column of ~ 120 m. Including the two moorings in the calculation results in an increase of the full MOC by ~ 0.2 Sv and a decrease of southward MFT by ~ 0.01 Sv.

Removal of M5 mooring in the central Irminger Sea. M5 was a deep mooring located near the center of the Irminger Sea along the OSNAP East line. It was deployed to cover the water column from 1500 m to the sea floor from August 2014 to June 2018. In the mean, M5 captured a northward velocity over its deployment period. To assess the impact of M5's removal, a comparison between the MOC estimates with and without the data from M5 for the deployment period was performed. The result indicates that removing M5 in the calculation leads to a strengthening of the mean MOC by 0.4 Sv. Our interpretation is that M5 measured a northward recirculation branch in the MOC lower limb that reduced the MOC estimate. For consistency with the first 4-year OSNAP calculation, we use the data from M5 in the MOC calculation from August 2014 to June 2018. After June 2018, no M5 data are available. Geostrophic velocity determined using mooring data on both sides of the original M5 position is used to fill the vacancy of M5.

Using directly measured velocity from moorings D1, D2 and D3 along the eastern flank of the Reykjanes Ridge. Moorings D1, D2 and D3 are located on the eastern flank of the Reykjanes Ridge in the Iceland Basin. Prior to 2018 they were configured for velocity and property measurements below 1200 m only. Velocity above 1200 m over the three moorings was calculated from geopotential height data provided by two tall moorings, one to the west and the other to the east. Starting in July 2018, the three moorings were extended to cover the entire water column, allowing for the use of direct velocity measurements in the MOC calculation. A comparison of the MOC estimates for July 2018 - June 2020 using geostrophic velocities with those using direct velocities shows that the latter results in a larger total MOC of just ~ 0.1 Sv. The MOC variability is similar for the two cases. This good agreement validates the application of end-point geostrophy over this region for the MOC estimate over the 2014-2018 period.

IB5 mooring replaced glider measurement over the Hatton-Rockall Basin. An additional mooring, IB5, was newly installed on the Hatton Bank along the OSNAP East section in July 2018. This mooring was added as a replacement for the discontinued glider observations with the last measurement in the Hatton-Rockall Basin in December 2017. IB5 is designed to capture the branch of the NAC in the Hatton-Rockall Basin with velocity and property measurements. A comparison between the MOC calculation with and without the IB5 data shows that its inclusion increases the mean MOC by ~ 0.5 Sv for the period from July 2018 to June 2020. A comparison of the MOC estimates with and without the glider data during the 2014-2017 period shows that including the glider data also increases the MOC by ~0.5 Sv. In light of the agreement between these two comparisons, we conclude that IB5 has adequately substituted for the glider measurements in the OSNAP observing system.

Recalibration of the 53°N array along the Labrador Sea western boundary and moorings M1, M2 and M3 along the Irminger Sea western boundary. A bias in the salinity data from the 53°N array at OSNAP West and in the Deep Western boundary moorings M1, M2 and M3 at OSNAP East for the period of August 2016 to June 2018 has been attributed to calibration error of the salinometer on board the cruise MSM74. MSM74 was responsible for the recovery and deployment of the moorings mentioned above in May and June 2018. To correct the bias in the mooring data, all affected salinities were increased by 0.004. This recalibration of the salinity data has only a minimum impact on the MOC. For both OSNAP East and OSNAP West, the difference in the mean MOC for the affected period is less than 0.1 Sv, much smaller than the uncertainties in the means.

References

[1] Li, F., M.S. Lozier, and W.E. Johns (2017): Calculating the Meridional Volume, Heat, and Freshwater Transports from an Observing System in the Subpolar North Atlantic: Observing System Simulation Experiment. *J. Atmos. Oceanic Technol.,* **34**, 1483–1500.

[2] Lozier, M. S., et al. (2019): A sea change in our view of overturning in the subpolar North Atlantic. *Science*, **363**, 516–521.

[3] Li, F., et al. (2021a): Subpolar North Atlantic western boundary density anomalies and the Meridional Overturning Circulation, *Nature Communications*, **12**, 1-9.

[4] Li, F., et al. (2021b): Observation-based estimates of heat and freshwater exchanges from the subtropical North Atlantic to the Arctic, *Progress in Oceanography*, **197**, 102640.

[5] Fu, Y. et al. (2023): Seasonality of the Meridional Overturning Circulation in the subpolar North Atlantic, *Communications Earth and Environment* (in revision).